Quantitative Evaluation of the Microsoft Kinect™ for Use in an Upper Extremity Virtual Rehabilitation Environment

Mason E. Nixon[1], Yu-Ping Chen[2], and Ayanna M. Howard[3]

[1,3]School of Electrical and Computer Engineering,
Georgia Institute of Technology, Atlanta, GA USA

[2]Department of Physical Therapy,
Georgia State University, Atlanta, GA USA

[1]*mnixon9@gatech.edu*, [2]*ypchen@gsu.edu*, [3]*ayanna.howard@ece.gatech.edu*

***Abstract*—Low cost depth sensors could potentially allow for home-based care and rehabilitation using virtual systems. Currently, no publicly available and peer-reviewed assessment has been made on the accuracy of joint position data determined by the Microsoft Kinect™ for assessment of upper extremity movements. We devised and validated clinically-based angle classifications for random arm movements in 3D-space, specifically, the shoulder joint flexion/extension angle, shoulder joint abduction/adduction angle, and 3-dimensional shoulder joint angle of 19 subjects at a distance of 2.0m using an eight camera Vicon Motion Capture system. Results show an average absolute error of these angle measurements not exceeding 10.0%.**

Keywords— Kinect; virtual; rehabilitation; evaluation; upper extremity; cerebral palsy; range of motion

I. INTRODUCTION

Rehabilitation after injury is crucial to recovery and to maintaining an adequate quality of life. Once a patient leaves clinical therapy, there remains a need for continuation of rehabilitation in the home [1], [2]. Many have also recognized the need for home-based rehabilitation programs to increase the quality of life in patients with other musculoskeletal conditions [1], [3], [4]. Engagement is key to an effective rehabilitation program and virtual systems are becoming more apparent as an effective means to this end [5], [6]. To decrease the load and increase the efficiency of physical or occupational therapists, home-based assessment shows promise. Inexpensive solutions in position determination such as the Microsoft (MS) Kinect ™ could be used by therapists to gain accurate and useful data on patient progress [7–9].

Virtual systems can be used to provide, not only the therapist with useful data, but also to give the patient much needed feedback on performance and encourage activity [6], [10–12]. Patients are able to immediately see feedback in a virtual environment. Virtual systems are also proving to be an effective means of functional recovery in upper limb rehabilitation [5], [6], [13]. Feedback on performance is crucial to motor learning and it is also an effective means of allowing for the patient to feel productive during the intervention [5].

This research was partially supported by the National Science Foundation under Grant No. 1208287 and the Grammy Foundation Grant Program. Any opinions, findings, and conclusions or recommendations expressed in this material are those of the authors and do not necessarily reflect the views of the National Science Foundation or the Grammy Foundation.

Currently, very expensive motion capture systems have been used in rehabilitation and other motion capture studies [7], [14], [15]. One such system is the Vicon camera system. The user must wear a non-infrared reflective suit with passive infrared (IR) reflective balls, or nodes, attached to it. The Vicon system uses multiple cameras to gain an accurate determination of the position of the nodes in 3D-space.

For home-based care, it would be extremely cost-prohibitive to utilize the Vicon system. On the other hand, the Kinect, a 3D depth camera, has the advantage of being relatively inexpensive and requires no special clothing or equipment to use. If proven to be accurate enough for use in therapeutic assessment, the Kinect could allow for a dramatic increase in the efficiency of therapists and the number of patients they can treat simultaneously, engagement of patients during home-based care, and quality of life for patients through its use in virtual rehabilitation.

II. PREVIOUS WORK

There have been some limited prior studies that have evaluated the accuracy of the Kinect with respect to rehabilitation scenarios. In [9], a very promising study was performed to demonstrate the accuracy of the Kinect sensor versus the Vicon, however, this study was limited to determining the position of stationary blocks. Previous work [8] determined human motion by comparing Kinect with Vicon, but was limited to only determining stride length. Although an assessment of the Kinect hardware versus another motion capture technology [7] has been performed (using the OptiTrack Optical Motion Capture System), it was recognized that a larger sample size and a larger variety of motion was still needed. Beyond these samples, to the best of our knowledge, there is currently no publicly available study that gives an assessment on the accuracy of the data provided by the Kinect sensor in upper extremity movements. Neither have we observed an existing markerless objective method of assessment for home-based rehabilitation. This paper attempts to fill in the gap by providing such an assessment.

III. EQUIPMENT

A. Kinect

The Kinect (or the underlying PrimeSense™ sensor [16]) consists of an infrared (IR) emitter (or projector), an IR depth sensor (IR camera), and an RGB sensor (camera) in addition to other unrelated hardware components (See Fig. 1). The emitter projects a speckle pattern of IR waves that are reflected off of objects which are then received by the IR depth sensor. These reflected waves create a new speckle pattern from which distances to objects may be determined by assessing the deformity of the new speckle pattern compared to the original. The technical specifications and details of the operation of the Kinect sensor can be found in observing the patents filed by PrimeSense [17–19]. The distances are used to form a depth image [20]. The Kinect for Windows SDK v.1.0.3.191 determines skeleton position information from the provided depth image. The result is Cartesian coordinates of joint positions related in meters with the Kinect depth sensor center as the origin (See Fig. 2). These skeletons can be acquired at a rate of about 20 to 26 samples per second which has been deemed more than adequate in determination of postures in industrial settings [21].

B. Vicon

The Vicon system used for this protocol consists of eight Vicon MX40 cameras (See Fig. 3) whose data are analyzed using the software ViconiQ v2.5 Build 275. Each camera has an array of IR lights that emit IR waves. These waves are reflected by the passive reflectors the subject is wearing at specific points on the body. The camera data is compiled in the Vicon 612 vR511 data station and then sent to a separate workstation with the ViconiQ software. The data from all 8 cameras is utilized to determine 3-dimensional positions of the reflectors. Once a capture session has been run, each passive IR reflector node must be labeled throughout the entire session. From this, the ViconiQ software generates a skeleton to fit within the nodes (See Fig. 4). After filtering the acquired data with a weighted average filter and a low pass Butterworth filter with an 8Hz cutoff and fitting the skeleton to each trial data, the result is position data of each joint in meters. The Vicon-generated skeleton joints do not all correspond exactly to the joints determined by the Kinect. For example, the Head joint compiled by the Vicon corresponds to the top of the head, while on the Kinect it is meant to represent the center of the head. Fortunately, in our study, we are only concerned with the shoulder flexion, shoulder abduction/adduction, and 3-dimensional shoulder angles. For this we only require the positions of the Center Shoulder, Shoulder, and Elbow joints (See Fig. 2). Since we know the origins of the Kinect skeleton and the Vicon skeleton coordinate systems we are able to perform a coordinate transformation so that we can compare the data from each sensor.

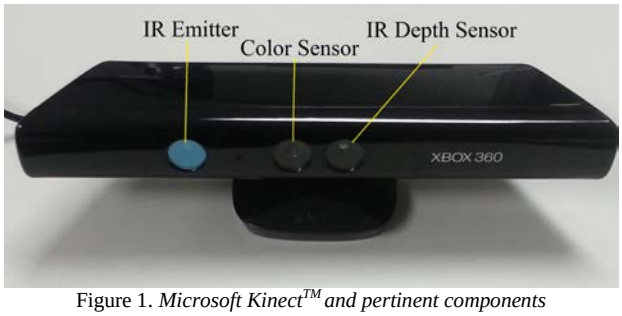

Figure 1. *Microsoft Kinect™ and pertinent components*

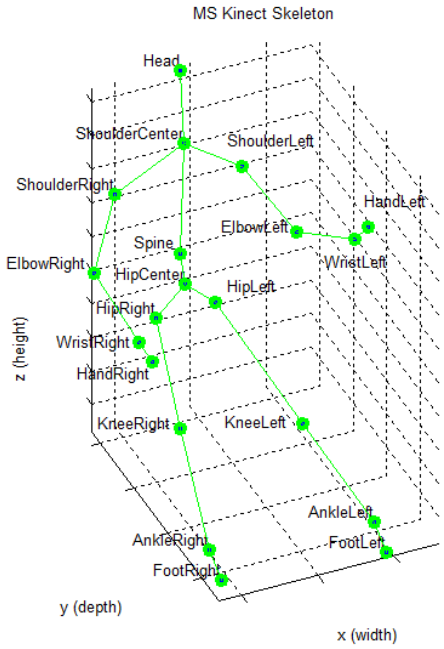

Figure 2. *Kinect skeleton and joints (in meters)*

IV. PROCEDURE

In order to confirm that the Kinect would be suitable for use with the SuperPop game, we assess its performance during game-play. For the evaluation, 19 participants (13 male and 6 female) were instructed to play the Super Pop VR™ game [22] wherein virtual bubbles are projected onto a screen in randomly dispersed locations (See Fig. 5). On the same screen, the participant sees a video stream of themselves in real time. The subjects are instructed to pop as many bubbles as they can in a 40 second time span. This procedure is repeated where the back of a stool on which the subject sits is placed at a distance of 2.0m from the Kinect.

V. DATA

The joint position determination algorithm provided by the Kinect was able to provide between 20 and 26 positions for each joint per second for a total of around 1,000 sample frames for each approximately 40 second timed trial. The Vicon yields exactly 100 joint positions per second for a total of usually 4,000 sample frames.

A. Filtering Method

For occluded or untracked joint positions, the Kinect algorithm must make an inference. Oftentimes the inference leads to what is characterized as spike noise in the data set. This spike noise, quantization noise, and other white noise associated with the sensor electronics must be filtered out

Figure 3. *Vicon MX camera*

before post-processing the data and determining joint angles since all subsequent calculations will amplify the noise.

We utilize what is typically used in the field for joint tracking data: a Butterworth filter [5], [23]. Particularly, a 6th order with a cutoff frequency of 3Hz. We choose 3 Hz through observation of the frequency content of our motion signal (Fig. 6). From the figure, some of the noise looks to be above 6 Hz, however, we achieve optimal results with the cutoff at 3 Hz. The Butterworth filter is an infinite impulse response (IIR) lowpass filter (LPF) [24]. Due to its recursive nature, this filter's impulse response extends for an infinite period of time. Butterworth filters are characterized as maximally flat, or with no ripple, in the passband [24]. As a 6th order Butterworth, our filter has a response with roll off of -36 dB per octave (-120 dB/decade) attenuation in the stopband.

B. *Filtering Results*

As seen in Fig. 7, our filter implementation is shown to have eliminated the high frequency noise components. The filtered Kinect data is much more correlated to the Vicon sensor data. Quantitative data associated with this error is provided in the results section.

C. *Angle Characterization*

We use the clinical definitions of arm motion to describe different types of arm ranges of motion we will measure in our study. Range of motion (ROM) is clinically defined based on the type of joint being measured. The shoulder joints are under

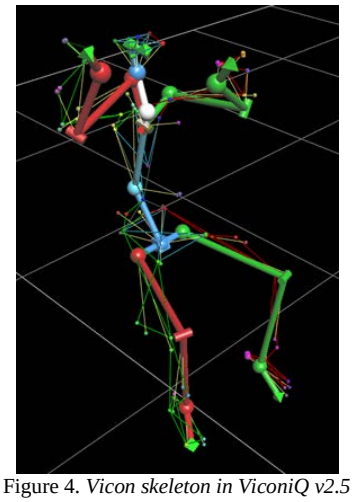

Figure 4. *Vicon skeleton in ViconiQ v2.5*

Figure 5. *Screen capture of Super Pop VR™ game-play with yellow square bubbles*

the classification of a synovial joint, which are joints in which the articulating bone ends are separated by a joint cavity containing synovial fluid [25]. Synovial joints are further sub-classified into other types based on the types of movements that are allowed by the joint. The shoulder is a part of the sub-class ball-and-socket joint which is a multiaxial joint wherein movement is allowed in all directions and pivotal rotation [25]. **Flexion** is a movement, typically in the sagittal plane (See Fig. 8), that decreases the angle of a joint and reduces the distance between the two bones of the joint. In contrast to this, **extension** is a movement that increases the angle of a joint and the distance between the bones [25]. **Abduction** is a movement of a limb away from the midline or median plane (a sagittal plane through the midline of the body), generally on the frontal, or coronal plane (See Fig. 8). In contrast, what is sometimes referred to as the opposite of abduction, **adduction** is movement toward the midline of the body [25]. The shoulder abduction/adduction ROM (which we will summarily refer to as just shoulder abduction) is defined as the point at which there is maximum abduction to the point at which there is maximum adduction (See Fig. 9). This can be thought of the arm motion used to make a snow angel. Shoulder flexion/extension ROM (again, summarily referred to as simply shoulder flexion) is defined as the point at which there is maximum flexion to the point where there is maximum extension of the arm at the shoulder joint (See Fig. 9). This can be thought of as the motion of the arm from rest in a standing position to straight up in the air, with the palm of the hand facing forward, as if to give a high five.

Since these clinical definitions of motion are restricted to motion on a fixed plane, we must derive our own classification

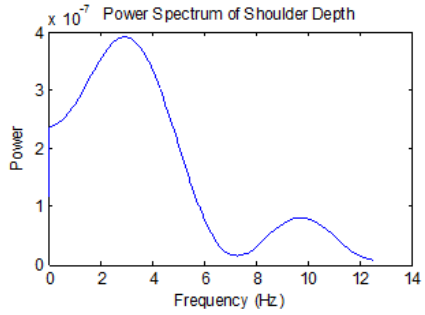

Figure 6. *Power Spectrum of Shoulder Depth*

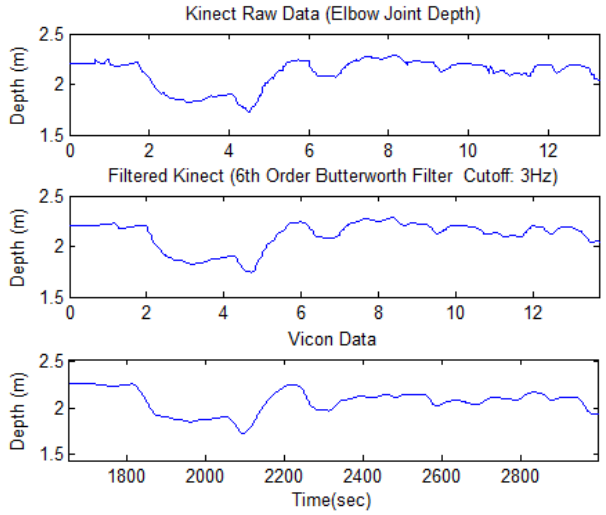

Figure 7. *A Comparison of Raw Kinect (Top), Filtered Kinect (Middle), and Vicon data (Bottom)*

for the unique motion that occurs in normal random reaching. We define our shoulder flexion angle as the angle of the shoulder made by projecting the upper arm onto a sagittal plane (perpendicular to the line made by the shoulder joint to the center shoulder joint) versus the coronal plane. Similarly, the shoulder abduction/adduction angle is defined as the angle formed by the upper arm projected onto the coronal plane versus the same sagittal plane used for flexion.

D. Angle Calculation

To calculate the 3-dimensional left and right shoulder angles, we simply determine the angle between the vector **s** created by the elbow joint and the shoulder joint and the vector **u** created by the shoulder joint and the center shoulder joint (See Fig. 2). Since we have the 3 Cartesian coordinates of the joints in 3D-space, we can create the vectors **s** and **u** and then compute the 3D angle, θ_{3D}, between the two vectors as seen in (1) [26].

$$\Theta_{3D} = \cos^{-1}(\boldsymbol{s}\cdot\boldsymbol{u} \,/\, |\boldsymbol{s}|\cdot|\boldsymbol{u}|) \tag{1}$$

Forming the clinical angles requires additional

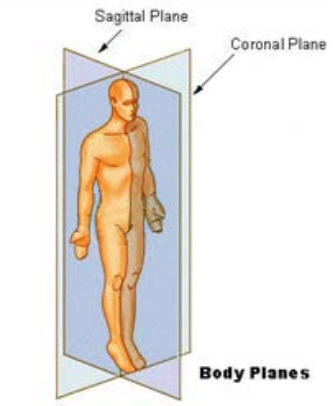

Figure 8. *The planes used to describe parts and actions of the body* [28]

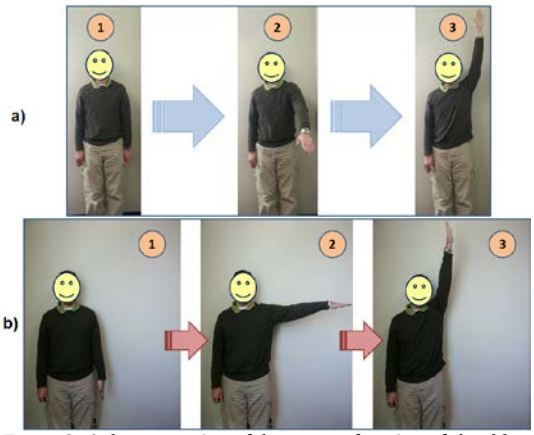

Figure 9. *A demonstration of the range of motion of shoulder flexion/extension (a) and shoulder abduction/adduction (b)*

computation. The shoulder abduction angle is created by projecting the upper arm onto a plane, D (which has a normal **m**), created by the cross product of shoulder vector **u** and upper spine vector **g** (See Fig. 2, Fig. 10 and (2)). The projection will be called vector **v**. The plane can be thought of a pseudo-coronal plane. After making the projection, we shift the upper spine to connect with the shoulder joint and call the shifted spine, vector **p**. The abduction angle can then be found by determining the angle between **v** and **p** using (1). Programmatically, we are solving the problem of intersecting a circle, C (whose radius is the upper arm with length d and has normal **n**: See (3)), and the plane D. If the point of intersection is P, then we are essentially solving for P as in (4). Since this will have 2 solutions, we choose the one closest to the elbow joint.

$$\boldsymbol{m} = \boldsymbol{u} \times \boldsymbol{g} \tag{2}$$

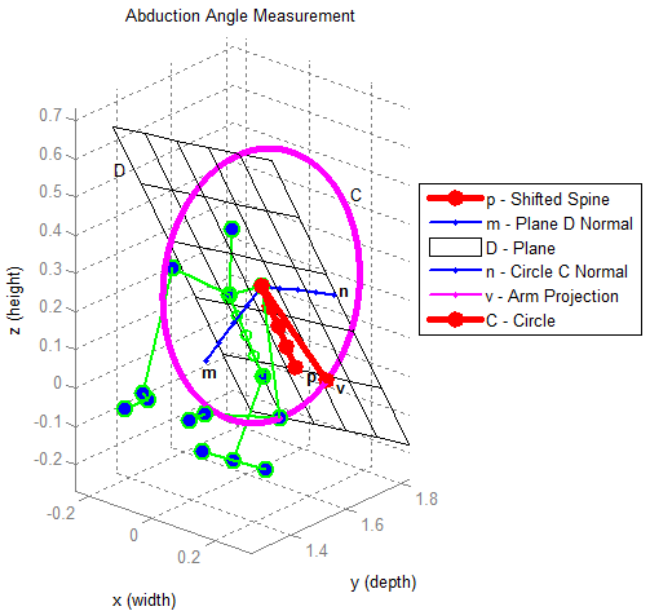

Figure 10. *The abduction angle calculation visualization (in meters)*

$$C = \boldsymbol{d}\cos(t)\cdot\boldsymbol{c} + \boldsymbol{d}\sin(t)\,(\boldsymbol{n}\times\boldsymbol{c}) + \mathrm{S}, \quad (3)$$

where S is the circle's centroid and **c** is an arbitrarily defined vector from S to the edge of circle C.

$$(C - P)\cdot\boldsymbol{m} = 0 \quad (4)$$

In a similar fashion as the abduction angle, we are able to determine the flexion angle. Here we are measuring the projection, vector **w**, against the same vector of the shifted spine, **p**. Vector **w** is formed by the point of the intersection of the circle with radius formed by the upper arm and with a normal perpendicular to **n** and the plane that is perpendicular to D and passes through the shoulder joint.

VI. Results

Since the two data sets between the Vicon and Kinect are not sampled at precisely the same time, to make a comparison we must design a method for correlating the data. To this effect, each subject was instructed to remain still until a countdown had completed. We use this time with a very low frequency of motion to line up the two data sets so that we may form a comparison. Since sample times also do not match up, we use the following metric (5) for determining the error between each arm trajectory, where a trajectory is defined as motion during the time between bubble pops in the virtual reality game.

We determine the average absolute error and the average absolute deviation for the shoulder angle range of motion (ROM) which is the difference of the maximum and minimum observed angles in a trajectory. We define absolute error (AE) as the percentage determined by the ratio of the difference in observed angles (Kinect: ROM_K, Vicon: ROM_V) and the theoretical maximum of the angles, which is 180 degrees (5). AE is averaged for each subject's trial and all subjects are then averaged (Reported as the solid bars in Fig. 11). The average absolute deviation is a measure of dispersion from the mean. It is found by finding the square root of the average of the variances.

$$AE = (|ROM_V - ROM_K| / 180)\cdot 100 \quad (5)$$

Table 1 shows the average absolute error of all trajectories of each subject for all 6 of our calculated angles. Fig. 11 represents a summary of Table 1 as well as the deviations from the means. From Fig. 11 we observe that the average absolute error does not exceed 10.0% for any of our angles. The Left Shoulder Abduction (LSA) angle error is 10.0%.The Right Shoulder Flexion (RSF) angle is 9.96%. The 3D Right (RS) and Left Shoulder (LS) angles are 6.81% and 7.64%, respectively. Right Shoulder Abduction (RSA) is 8.18% and Left Shoulder Flexion (LSF) is 9.31%. The average absolute deviations are highest on the LSA (10.6%) and RSF (11.2%) and lowest on LS (7.28%) and RS (6.33%). The LSF and RSA were 10.3% and 9.33%, respectively. Our highest deviations were observed in trajectories where we note occlusions of joint positions in the Vicon data. The error was higher for the angles which were determined from the original positions using many calculations such as LSA, LSF, RSA, and RSF. This fits our intuition since we propagate the error in the position measurements when performing further calculations.

TABLE I. Summary of Average Absolute Error of All Trajectories

	LSA (%)	LSF (%)	RSA (%)	RSF (%)	LS (%)	RS (%)
Subject1	7.11	8.74	5.24	14.88	6.22	8.86
Subject2	8.63	6.21	3.50	5.92	7.15	6.26
Subject3	10.78	6.38	11.24	8.69	9.67	6.29
Subject4	3.96	3.49	3.88	4.58	2.89	3.53
Subject5	4.75	5.51	7.10	8.22	6.43	7.13
Subject6	6.89	8.16	5.29	6.25	7.05	6.12
Subject7	7.43	8.56	7.77	14.79	5.89	5.67
Subject8	12.47	14.00	8.09	20.43	10.51	9.46
Subject9	8.65	16.78	12.30	9.81	6.10	9.26
Subject10	9.06	10.02	12.69	7.48	10.26	8.18
Subject11	8.10	7.07	6.30	8.77	6.40	5.78
Subject12	15.51	12.12	4.06	6.81	7.01	7.08
Subject13	12.47	9.36	8.36	6.20	10.29	5.11
Subject14	8.19	10.35	10.49	8.74	6.65	6.43
Subject15	9.23	11.93	9.23	8.30	9.91	7.07
Subject16	10.96	9.18	11.38	11.63	10.74	7.25
Subject17	15.01	7.21	10.29	8.29	5.47	5.82
Subject18	9.43	7.85	6.01	15.79	6.18	5.76
Subject19	22.17	14.00	12.18	13.68	10.39	8.31

VII. Discussion

We have termed and validated clinical angle measurements that can be used to classify motion of the arm. Using these angle definitions, everyday arm motion may more easily be quantitatively defined and assessed for therapeutic purposes.

When assessing the results, one must also consider the method of angle determination as a source of error. Although the Kinect and Vicon skeletons both are formed through estimation of the centroid of joint positions, they have not been determined to be precisely identical (See Fig. 2 & Fig. 4) and so one source of error may also be in the difference in joint coordinates.

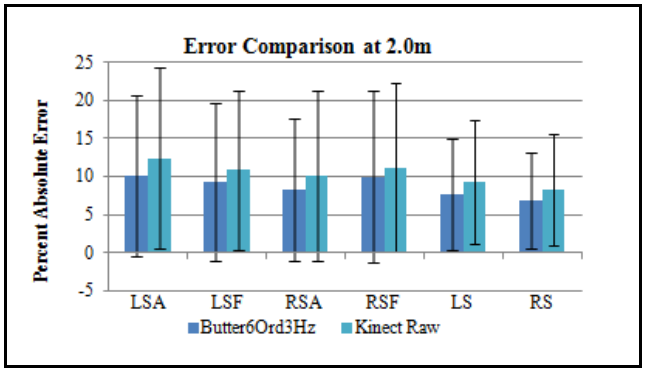

Figure 11. *The plot shows the average percent absolute error comparison at 2.0m of 6th order Butterworth filter with a 3 Hz cutoff frequency (leftmost bars) and the raw Kinect data (rightmost bars) each versus the Vicon data for all 19 subjects. The vertical line bars represent +/- the average absolute deviation.*

Currently, to the best of our knowledge, there is no markerless method for quantitative assessment in the home environment. Furthermore, most practicing (non-research) clinical assessments are based on subjective measures (PDMS-2, Fugl-Meyer, GMFM, etc.) [27]. In this research, we have shown preliminary results that validate the utilization of an objective assessment method to be used in home-based and non-research based rehabilitation. These results are believed to be indicative of the potential usage of the Kinect in a virtual rehabilitation system. As a direct result, home-based therapy can then be used to provide quantitative feedback to patients and therapists in an inexpensive way. We believe that in-home clinical systems that can measure kinematics without specialized markers or gloves open the field to a new domain. By using such systems, therapists could treat many more patients and increase their overall efficiency. Through more meaningful feedback, patients can not only gain functional recovery much more expeditiously, but also increase their aptitude for motor learning and perhaps see an increase in engagement. All this ultimately leads to a better patient quality of life.

VIII. Conclusions & Future Work

From this assessment, we have formed a quantitative measure of the accuracy of the MS Kinect for the shoulder flexion angle, shoulder abduction/adduction angle, and the 3-dimensional shoulder angle observed in random reaching activities. We have also created a method for translating reach into measurable clinically-based shoulder angles.

We recognize that improvements can be made in the filtering of the data. Further exploration should be made in filtering methods. We also recognize that many other parameters could be evaluated from the acquired data from our assessments. This will form the basis of our future work in this area.

Acknowledgment

We would like to thank Dr. Magnus Egerstedt and his team in the Georgia Tech GRITS lab for their support through use of their Vicon camera system and motion capture lab.

References

[1] D. L. Wong, “Diseases of Muscles,” in *Wong’s Nursing Care of Infants and Children*, 9th ed., vol. 4, no. 1, M. J. I. Hockenberry and D. Wilson, Eds. St. Louis, MO: Elsevier Mosby, 2011, pp. 1689–1730.

[2] B. Dow, K. Black, F. Bremner, and M. Fearn, “A comparison of a hospital-based and two home-based rehabilitation programmes.,” *Disability and rehabilitation*, vol. 29, no. 8, pp. 635–641, 2007.

[3] M. Katz-Leurer, H. Rotem, O. Keren, and S. Meyer, “The effects of a ‘home-based’ task-oriented exercise programme on motor and balance performance in children with spastic cerebral palsy and severe traumatic brain injury.,” *Clinical Rehabilitation*, vol. 23, no. 8, pp. 714–724, 2009.

[4] P. Stolee, S. N. Lim, L. Wilson, and C. Glenny, “Inpatient versus home-based rehabilitation for older adults with musculoskeletal disorders: a systematic review.,” *Clinical Rehabilitation*, vol. 26, no. 5, pp. 387–402, 2011.

[5] Y.-P. Chen, L.-J. Kang, T.-Y. Chuang, J.-L. Doong, S.-J. Lee, M.-W. Tsai, S.-F. Jeng, and W.-H. Sung, “Use of virtual reality to improve upper-extremity control in children with cerebral palsy: a single-subject design.,” *Physical therapy*, vol. 87, no. 11, pp. 1441–57, Nov. 2007.

[6] M. Levin and L. Knaut, “Virtual reality environments to enhance upper limb functional recovery in patients with hemiparesis,” *Studies In Health Technology And Informatics*, vol. 145, pp. 94–109, 2009.

[7] C.-Y. Chang, B. Lange, M. Zhang, S. Koenig, P. Requejo, N. Somboon, A. Sawchuk, and A. Rizzo, “Towards Pervasive Physical Rehabilitation Using Microsoft Kinect,” *Proceedings of the 6th International Conference on Pervasive Computing Technologies for Healthcare*, pp. 2–5, 2012.

[8] E. Stone and M. Skubic, “Evaluation of an Inexpensive Depth Camera for Passive In-Home Fall Risk Assessment,” *Proceedings of the 5th International ICST Conference on Pervasive Computing Technologies for Healthcare*, 2011.

[9] T. Dutta, “Evaluation of the Kinect™ sensor for 3-D kinematic measurement in the workplace.,” *Applied ergonomics*, vol. 43, no. 4, pp. 645–9, Jul. 2012.

[10] M. J. D. Taylor, D. McCormick, T. Shawis, R. Impson, and M. Griffin, “Activity-promoting gaming systems in exercise and rehabilitation,” *The Journal of Rehabilitation Research and Development*, vol. 48, no. 10, p. 1171, 2011.

[11] A. De Mauro, “Virtual Reality Based Rehabilitation and Game Technology,” *EICS4Med 2011*, vol. i, pp. 48–52, 2011.

[12] K. Jordan and M. Sampson, “ImAble system for upper limb stroke rehabilitation,” in *International Conference on Virtual Rehabilitation*, 2011, pp. 1–2.

[13] M. Sandlund, H. Grip, C. Hager, E. Domellof, and L. Ronnqvist, “Low-cost motion interactive video games in home training for children with cerebral palsy: A kinematic evaluation,” in *International Conference on Virtual Rehabilitation*, 2011, pp. 1–2.

[14] D. S. Stokic, T. S. Horn, J. M. Ramshur, and J. W. Chow, “Agreement between temporospatial gait parameters of an electronic walkway and a motion capture system in healthy and chronic stroke populations.,” *American journal of physical medicine rehabilitation Association of Academic Physiatrists*, vol. 88, no. 6, pp. 437–444, 2009.

[15] S. Thies, P. Tresadern, L. Kenney, D. Howard, J. Goulermas, C. Smith, and J. Rigby, “Comparison of linear acceleration from three measurement systems during “reach & grasp,” *Medical Engineering & Physics*, vol. 29, no. 9, pp. 967–972, 2007.

[16] L. PrimeSense, “PrimeSense 3D Sensors,” *Developers > Get Your Sensors*, 2013. [Online]. Available: http://www.primesense.com/developers/get-your-sensor/. [Accessed: 02-May-2013].

[17] B. Freedman, A. Shpunt, M. Machline, and Y. Arieli, “Depth Mapping Using Projected Patterns,” U.S. Patent 20100118123.

[18] A. Shpunt, “Depth Mapping Using Multi-beam Illumination,” U.S. Patent 20100020078.

[19] E. Spektor, Z. Mor, and D. Rais, “Integrated Processor for 3D Mapping,” U.S. Patent 20100007717.

[20] Microsoft Corporation, “Kinect for Windows Sensor Components and Specifications,” *MSDN*, 2010..

[21] D. M. Andrews and J. P. Callaghan, “Determining the minimum sampling rate needed to accurately quantify cumulative spine loading from digitized video.,” *Applied Ergonomics*, vol. 34, no. 6, pp. 589–595, 2003.

[22] S. García-Vergara, A. Howard, and Y. Chen, “Super Pop VR: an Adaptable Virtual Reality Game for Upper-Body Rehabilitation,” in *15th International Conference on Human-Computer Interaction*, 2013.

[23] D. a Winter, H. G. Sidwall, and D. a Hobson, “Measurement and reduction of noise in kinematics of locomotion.,” *Journal of biomechanics*, vol. 7, no. 2, pp. 157–159, Mar. 1974.

[24] Analog Devices, “IIR Filter Design Techniques,” in *Mixed-Signal and DSP Design Techniques*, W. Kester, Ed. Burlington, MA: , 2003, pp. 173–176.

[25] E. M. Marieb and S. J. Mitchel, *Human Anatomy & Physiology*, 9th ed. San Francisco, CA: Pearson Benjamin Cummings, 2009, pp. 169–186.

[26] J. Stewart, “Vectors and the Geometry of Space,” in *Calculus*, 7th ed., L. Covello, Ed. Belmont, CA: Brooks/Cole, Cengage Learning, 2012, pp. 809–857.

[27] E. E. Butler, A. L. Ladd, S. a Louie, L. E. Lamont, W. Wong, and J. Rose, “Three-dimensional kinematics of the upper limb during a Reach and Grasp Cycle for children.,” *Gait & posture*, vol. 32, no. 1, pp. 72–7, May 2010.

[28] U. S. National Institutes of Health: National Cancer Institute, “SEER Training Modules,” *Anatomical Terminology*, 2006.